

Performance Analysis of Statistical Parameter Based Fire Pixel Segmentation in Various Color Spaces

¹C. Emmy Prema and ²S.S. Vinsley

¹Department of Electronics and Communication Engineering,
Bethlahem Institute of Engineering, 629157 Karungal, Tamil Nadu, India

²Department of Electronics and Communication Engineering,
Lourdes Mount College of Engineering and Technology, 629195 Marthandam,
Tamil Nadu, India

Abstract: In this study the performance of fire pixel segmentation technique is analysed in RGB, YUV, CIE L*a*b* and YCbCr color spaces using statistical parameters of the image. Various rules are formed in each color space by defining color and texture feature of the fire and also research is carried out to segment the fire centre region. The true fire pixels including fire flame region and fire centre region are effectively segmented from the background in YCbCr color space than the other color spaces. The fire pixel segmentation method using static features of fire (Color and texture) is less complex than dynamic features of fire like motion, flickering, rate of growing etc. and can be incorporated in the situation when the camera is moving.

Key words: Fire segmentation, color space, fire pixel, statistical parameters, India

INTRODUCTION

Now a days one of the most important surveillance systems is the fire detection system used to monitor the environments and buildings. Fire is the most common hazard affecting everyday life around the world. Forest fire is very harmful to forests and results in very serious economic losses. Timely and accurate fire detection are crucial to avoid large scale fire damage. If a fire is detected as early as possible, then the chances for survival are better. It is also necessary for the clear understanding of the fire development and the location. Initial fire locations, the size of the fire, fire growing rate and direction of smoke propagation are the important parameters for firefighting and essential for fire safety analysis. Almost all the fire detection systems use built-in sensors. The reliability of such system depends on the positional distribution of sensors. Sensors are limited to indoors and not applicable to outdoors such as forests, shopping centres, railway stations etc. They require close proximity to fire which could damage the sensor and also need frequent battery charge. These sensors do not provide any information about the fire location, size, growing rate etc.

Due to rapid development of digital camera technology and video processing technology, all the conventional fire detection systems are replaced by a

video processing technique which uses a digital video camera (Celik *et al.*, 2006). Now a days millions of digital video cameras are installed all over the world. But it is impractical for the operator to keep a constant eye on every single camera. The performance of fire detection system depends on the performance of fire pixel classifier which generates the seed areas on which the rest of the system operates. The detection rate of fire pixel classifier is needed to be very high with less false alarm rate. There exists a different technique in different color spaces to segment fire pixel described in the literature.

Celik *et al.* (2006) proposed a generic color model to segment the flame pixel from the background using the YCbCr color model. This method segments the flame region except the flame centre. Chen *et al.* (2004) developed a set of rules to separate the fire pixels using R, G and B information. It will not respond correctly when the illumination of the image changes. Toreyin *et al.* (2005) used a mixture of Gaussians in RGB color space which is developed from a training set of fire pixels, instead of using a rule-based color model as Chen *et al.* (2004). Toreyin *et al.* (2006) employed a hidden markov models to detect the motion characteristics of the fire flame that is fire flickering along with the fire pixel classification. Celik *et al.* (2007) formed number of rules using normalized (rgb) values in order to avoid the effects of changing illumination. In this method, statistical

analysis is carried out in rg, rb and gb planes. In each plane three lines are used to specify a triangular region representing the region of interest of fire pixels. A pixel is declared as fire pixel if it falls in the triangular region of rg, rb and gb planes. Even though the normalized RGB color space overcomes the effects of variation in illumination to some extent, further improvement can be achieved by using YCbCr color space which separates luminance from chrominance. Marbach *et al.* (2006) used YUV color space for the analysis of video data. In this technique time derivative of Y component is used to segment the candidate fire pixel and U and V components are used to extract the features of segmented fire pixel and confirm whether the segmented fire pixel is in the fire region.

Hornig *et al.* (2005) used HSI color model to separate the fire pixels. They have developed the rules for brighter and darker environments. After segmenting the fire region based on HSI rules, the lower intensity and lower saturation pixels are removed to avoid fire aliases (fire like region). They have also formed a metric based on binary counter difference images to measure the burning degree of fire flames such as no fire, small, medium and big fires. Their result includes false positives and false negatives. But there is no way to reduce the false positives and false negatives by changing their threshold value. Ko *et al.* (2009) generates RGB probability model using unimodal Gaussian function from a set of sample images containing fire to segment the fire pixels based on color. But some of the non-fire pixels similar color to fire probability model is also detected as fire pixels.

Celik (2010) proposed a fast and efficient fire detection using CIE $L^*a^*b^*$ color space. They have introduced different types of concepts to reduce the false alarm rate. $L^*a^*b^*$ color space is perceptually uniform and it is possible to represent the color information of fire better than the other color spaces. It incorporates the mean value of the image in L^* , a^* and b^* plane and also the histogram of fire pixel is created for each of the planes to separate fire image from the background. But the major limitation is that it cannot differentiate smoke from fire flame. Vipin (2012) proposed a model to segment the fire from the image which uses RGB and YCbCr color space. This method does not research well under all environmental conditions and is not reliable. Patel and Tiwari (2012) and Jin and Zhang (2009) used combined approach of color detection, motion detection and area dispersion to detect fire in video. Color-based detection is achieved by analyzing fire in RGB and YCbCr color model. The accuracy of this technique is greatly reduced when the background illumination changes and it also segments clouds as fire centre region (white).

Celik *et al.* (2007) used different color models to detect fire and smoke. Specifically, fuzzy rules are

generated in YCbCr color space to detect fire flame. It is better in discriminating fire from fire-like colored objects but it missed to segment the fire centre region. Hornig *et al.* (2005) proposed fire and flame detection method by processing a video data. Here the analysis is carried out in RGB and HSI color space. Spatial variation of color component in HSI color space is used to separate fire flame. Also conversion from RGB to HSI is not linear; hence it is a time consuming process. Xie *et al.* (2009) and Stadler and coauthors proposed an algorithm to segment the fire central area of boiler flame in YCbCr color space. In this method segmentation is done effectively but it does not segment the fire flame area (around central area) which is the major area of the fire. Li and coauthors describes an algorithm to measure the relevance of color context of every two adjacent frame of flame image sequences. This algorithm uses image's statistical parameters in RGB color space. Chen *et al.* (2004) proposed a fire detection algorithm using CIE $L^*a^*b^*$ and YCbCr color space. It uses a threshold value for chrominance components (Cb and Cr) in YCbCr color space. These threshold values depend on background illumination. Even though many researchers carried out the research to segment fire in various color spaces, the centre fire region is not effectively segmented. But the proposed research in YCbCr color space, segment fire centre region by defining texture of the fire using statistical parameter of the image.

MATERIALS AND METHODS

Fire segmentation techniques using color model: The method by which color is specified, created and visualized color is called color space. Human beings define color by its attribute of brightness, hue and colorfulness. A computer may describe a color using the amount of red, green and blue phosphor emission required to match a color. A color is specified using three co-ordinates or parameters. These parameters give the position of color within a color space being used. Many different color spaces are used for fire detection. Each color space differs from the others in terms of transformation (linear or non-linear), the robustness to adapt to light changing and shadow noises. In this study analysis is carried out in RGB, YUV, CIE $L^*a^*b^*$ and YCbCr color spaces.

Analysis in RGB color space: RGB color model is used for sensing, representation and display of images in electronic systems such as television and computers. It is based on human perception of colors and it does not decouple color from intensity. Digital video camera also provides the output in RGB color space. RGB color space



Fig. 1: Input image with R, G and B components; a) Input image; b) R component; c) G component and d) B component

is the basic color space from which other color spaces are derived. It is the combination of three basic colors (Red, Green and Blue). Each digital color image has three color planes: Red (R), Green (G) and Blue (B). Each color plane is quantized into discrete levels, generally 256 (8 bits per color plane) and quantization levels are used for each plane. White color is represented by $(R, G, B) = (255, 255, 255)$. Black is represented by $(R, G, B) = (0, 0, 0)$. A color image consists of a pixel; each pixel is represented by spatial location in the rectangular grid (x, y) . $(R(x, y), G(x, y), B(x, y))$ is the color vector corresponding to the spatial location (x, y) . Thus, the camera provides the image in RGB color space.

Rules in RGB color space: In the fire region of the digital fire image, the value of red channel (R) is greater than the value of green channel (G) (Elik and Demirel, 2009; Toreyin *et al.*, 2006). In order to explain this concept clearly, some sample images are picked and R component, G component and B component are separated as shown in Fig. 1a. From Fig. 1b-d), it can be noticed that, in the fire region the intensity of Fig. 1b) (R component) is greater than Fig. 1c, (G component) and the intensity of Fig. 1c, (G component) is greater than Fig. 1d) (B component). In some images, non-fire regions may also have higher R

component than G component and higher G component than B component. It results in the segmentation of some of the non-fire pixels as fire pixel. In order to overcome this limitation the mean value of image is calculated for R plane (R_{mean}). It is confirmed that the value of R component in fire regions of the input image is greater than R_{mean} for the same image. This concept is explained through the graph shown in Fig. 2 with $\lambda = 127$. For the pixels in the fire region, R component is more than R_{mean} and for the pixels in the non-fire region R component is less than R_{mean} . Based on the points discussed the following rules are formed in RGB color space:

$$R_{RGB1}(x, y) = \begin{cases} 1, & \text{if } R(x, y) > G(x, y) > B(x, y) \\ 0 & \text{otherwise} \end{cases} \quad (1)$$

$$R_{RGB2}(x, y) = \begin{cases} 1, & \text{if } R(x, y) > R_{mean} \\ 0 & \text{otherwise} \end{cases} \quad (2)$$

where, R_{RGB1} and $R_{RGB2}(x, y)$ are the pixels satisfying the conditions given in Eq. 1 and 2, respectively. R_{mean} is the mean of pixel intensity in R plane and if there are $M \times N$ number of pixels in the given image then R_{mean} can be calculated using Eq. 3 as follows:

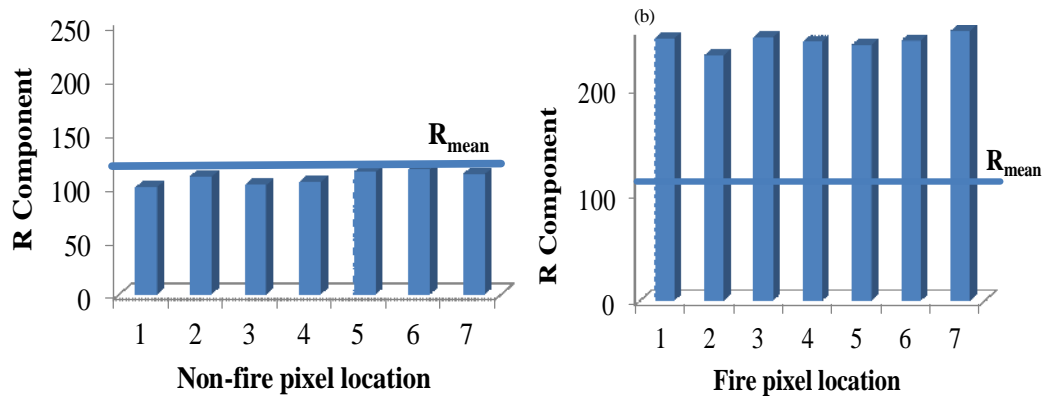


Fig. 2: Intensity of R component in different pixel locations; a) Fire; b) Non-fire pixels

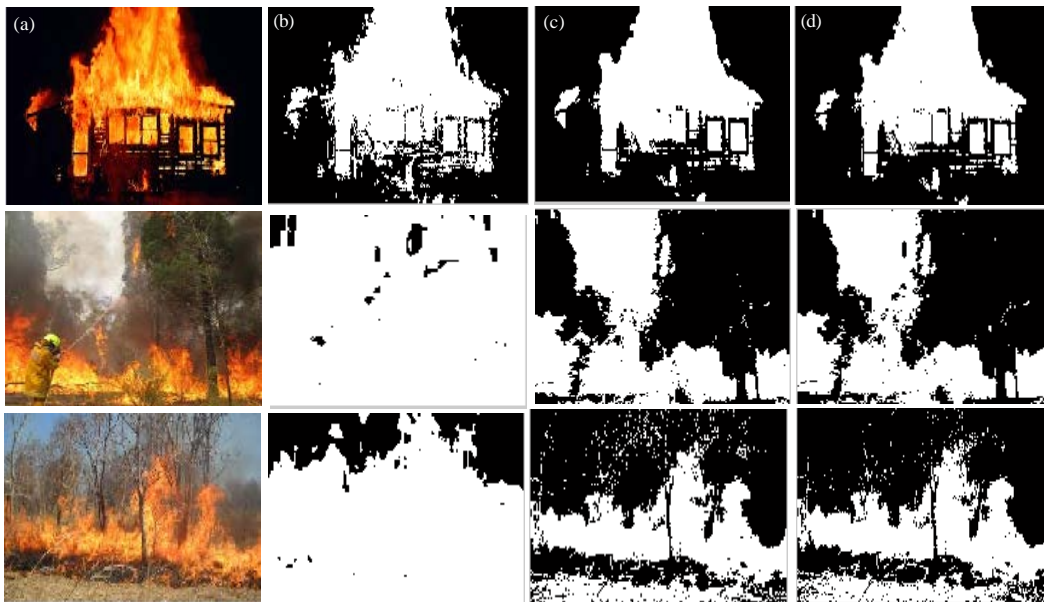


Fig. 3: Results observed in RGB color space; a) Input RGB image; b) Fire segmentation using Eq. 1; c) Fire segmentation using Eq. 2 and d) True fire segmentation using Eq. 4

$$R_{\text{mean}} = \frac{1}{M \times N} \sum_{x=1}^M \sum_{y=1}^N R(x, y) \quad (3)$$

Finally, true fire pixels using RGB color space is considered as the pixels satisfying both Eq. 1 and 2:

$$R_{\text{RGB}}(x, y) = \begin{cases} 1(x, y), & \text{if } R_{\text{RGB1}}(x, y) = 1 \text{ and } R_{\text{RGB2}}(x, y) = 1 \\ 0 & \text{otherwise} \end{cases} \quad (4)$$

where, (x, y) is the pixel of input image at the location (x, y) and $R_{\text{RGB}}(x, y)$ is the true fire pixel segmented in RGB color space. $R_{\text{RGB}}(x, y)$ exists if and only if the pixel in the location (x, y) satisfies the conditions given in Eq. 1

and 2. To segment the fire pixels in the RGB color space, the mean value of R component is taken as statistical parameter because in each fire pixel R component plays a vital role.

Performance in RGB color space: RGB color model is used in all the fire detection systems because almost all the visible range cameras have sensors detecting videos in RGB format. The result of Eq. 1, 2 and 4 are shown in Fig. 3. In Fig. 3b, few non-fire pixels are identified as fire pixels, because those non-fire pixels also satisfy the condition given in Eq. 1. Similarly, in Fig. 3c non-fire cloud is segmented as fire by satisfying Eq. 2. Fig. 3d shows the true fire pixels satisfying Eq. 4. It can be noted that for row

2 and 3 of Fig. 3, background illumination is high. Due to this high background illumination some of the non-fire regions (cloud and fire shaded regions) are also segmented as fire. Even though RGB color space can be used for fire pixel segmentation, it has a disadvantage of luminance dependence. That is when the illumination of input image changes, it exhibits inaccurate results. This is due to the high correlation between R, G and B components of RGB color space. Also in RGB color space, luminance and chrominance information are mixed.

RESULTS AND DISCUSSION

Analysis in YUV color space: YUV color space uses only one luma (luminance component) called Y component and two chrominance components called U and V components. It encodes the color image and allows reduced bandwidth for chrominance component. In YUV colour space, there is no correlation between Y, U and V components. It is also very simple to compute it from the RGB color space. Conversion from RGB-YUV colour space is Eq. 6 as in Eq. 5:

$$\begin{bmatrix} Y \\ U \\ V \end{bmatrix} = \begin{bmatrix} 0.299 & 0.587 & 0.114 \\ -0.14713 & -0.28886 & 0.436 \\ 0.615 & -0.51499 & -0.10001 \end{bmatrix} \begin{bmatrix} R \\ G \\ B \end{bmatrix} \quad (5)$$

Range of Y is from 0-255; the range of U is from 0 to ± 112 and of the V is from 0 to ± 157 .

Rules in YUV colour space: In the input image containing fire and non-fire pixels, each pixel value is analysed deeply in each color plane (Y, U and V) of the YUV color space. While comparing the intensity of Y (Y component), U (U component) and V (V component), intensity of Y component is far greater than the intensity of U component and the intensity of V component is greater than U component for fire pixels.

But for non-fire pixels U component value is greater than V component. The concept described above is shown in Fig. 4. In the YUV color space Y component describes the luminance property.

Fire is a light source which exhibits higher luminance than other non-fire regions which means that fire pixels have higher value of Y component. Also V component of the pixel differs more in between fire and non-fire regions. Even though U and V are chrominance components, the intensity of V component is more than the intensity of U in the fire pixels. At the same time, some of the fire like light sources (i.e, sun, fire reflection, light of vehicle, etc.) also exhibit the same color characteristics as fire pixels. This will lead to fire aliases. To overcome this complexity, texture feature of the fire is considered by incorporating

Table 1: Fire and non-fire pixel values in Y, U and V planes along with Y_{mean} and V_{std}

$Y_{mean} = 87.932$ and $V_{std} = 11.96$					
Fire pixel			Non fire pixel		
Y	U	V	Y	U	V
237	55	15	70	31	1
224	36	17	147	59	4
225	35	36	122	52	3
230	34	22	90	36	6
182	27	63	109	44	3

the mean of the image in Y plane (Y_{mean}) and standard deviation of the image in V plane (V_{std}). From Table 1, it is clear that pixels in the fire region have greater V component than (V_{std}) and the pixels in non-fire region have less V component value than (V_{std}). In the same way Y component is greater than (Y_{mean}) for the pixels in the fire region and is less than (Y_{mean}) for the pixels in the non-fire region. These conditions are verified for more than thousand images and is formulated as three rules given below:

$$R_{YUV1}(x, y) = \begin{cases} 1, & \text{if } Y(x, y) > U(x, y) < V(x, y) \\ 0 & \text{otherwise} \end{cases} \quad (6)$$

$$R_{YUV2}(x, y) = \begin{cases} 1, & \text{if } Y(x, y) > Y_{mean} \text{ and } V(x, y) > V_{std} \\ 0 & \text{otherwise} \end{cases} \quad (7)$$

where, $R_{YUV1}(x, y)$ and $R_{YUV2}(x, y)$ are the pixels satisfying Eqs. 6 and 7, respectively. Y_{mean} and V_{std} are the mean and standard deviation of image in Y and V plane, respectively. $y(x, y)$, $U(x, y)$ and $V(x, y)$ are the intensity of each pixel at location (x, y) in Y, U and V plane, respectively. The formulas to calculate Y_{mean} and V_{std} are given in Eq. 8 and 9, respectively:

$$Y_{mean} = \frac{1}{M \times N} \sum_{x=1}^M \sum_{y=1}^N Y(x, y) \quad (8)$$

$$V_{std} = \sqrt{\frac{1}{M \times N} \sum_{x=1}^M \sum_{y=1}^N (V(x, y) - V_{mean})^2} \quad (9)$$

where, $M \times N$ is the total number of pixels in the given image:

$$V_{mean} = \frac{1}{M \times N} \sum_{x=1}^M \sum_{y=1}^N V(x, y)$$

Finally, true fire pixels using YUV color space are determined by considering those pixels satisfying all the above mentioned rules Eq. 6 and 7 and it is given by:

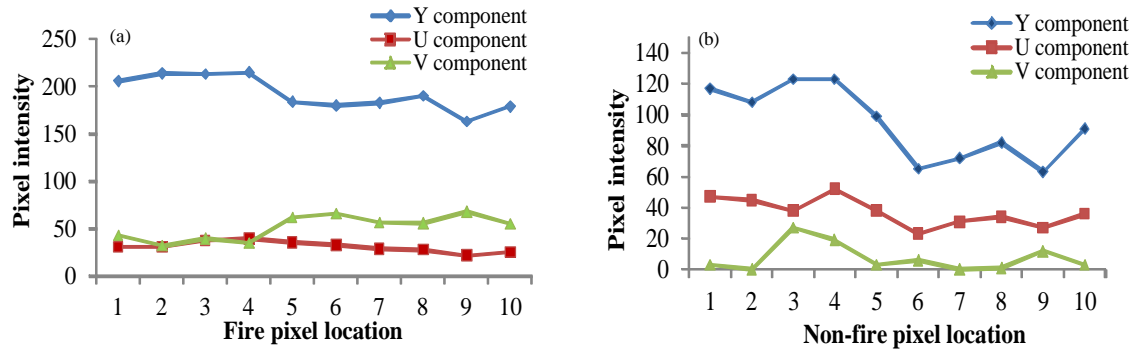


Fig. 4: Distribution of Y, U and V components in fire and non-fire regions

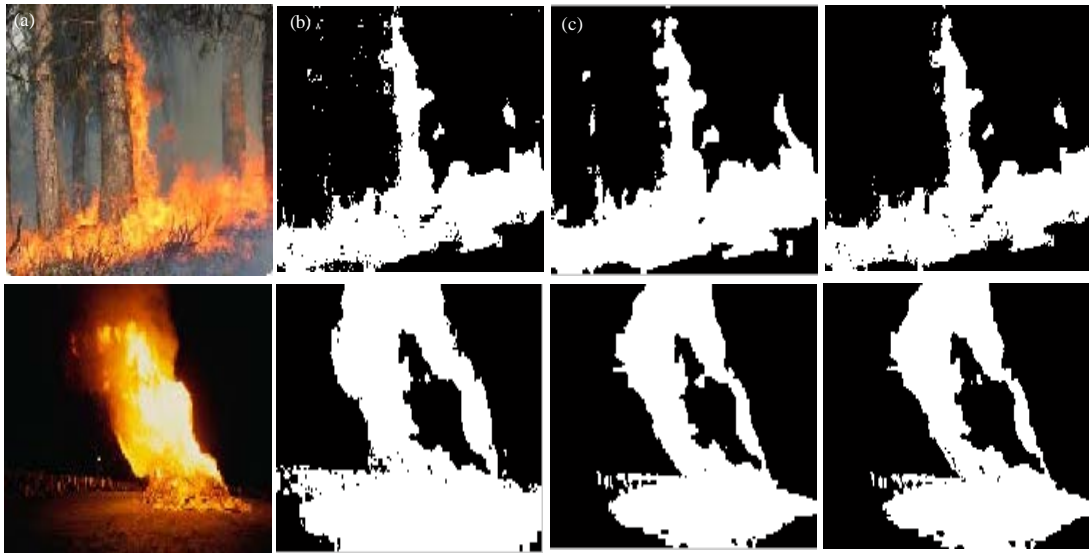


Fig. 5: Result of fire pixel segmentation in YUV color space; a) Input image; b) Segmented fire pixels using Eq. 6; c) Segmented fire pixels using Eq. 7 and d) Segmented fire pixels using Eq. 10

$$R_{YUV}(x,y) = \begin{cases} I(x,y), & \text{if } R_{YUV1}(x,y) = 1 \text{ } R_{YUV2}(x,y) = 1 \\ 0 & \text{otherwise} \end{cases} \quad (10)$$

Where:

$I(x,y)$ = The intensity of input RGB image at the location (x,y)

R_{YUV} = The fire pixel segmented as fire pixel in YUV color space

Performance in YUV color space: Fire region segmented using Eq. 6, 7 and 10 is shown in Fig. 5. In second row of Fig. 5, the centre fire region is not segmented as true fire since centre region of fire is at very high temperature which exhibits white color. Even though the standard deviation of image (V_{std}) involves image’s texture feature, white colored fire center region is not separated as fire using YUV color space.

Analysis in CIE L*a*b* color space: The International Common on Illumination (CIE) introduced L*a*b* color space which is perceptually uniform: that means the change of same amount of color value should produce a change of same visual importance. Two colors which appear similar to a human observer lie very close in the CIE L*a*b* color space. In this color space one can take into account of the illumination character of the image. CIE L*a*b* color space is a device independent because it is independent of the device which produces and displays the image.

In CIE L*a*b* color space L* represents the lightness which indicates the level of light or dark; a* encodes red and green sensation with positive value of a* indicating a* as red color and negative value of a* indicating a* as an green color; b* encodes yellow and blue sensation with positive value of b*

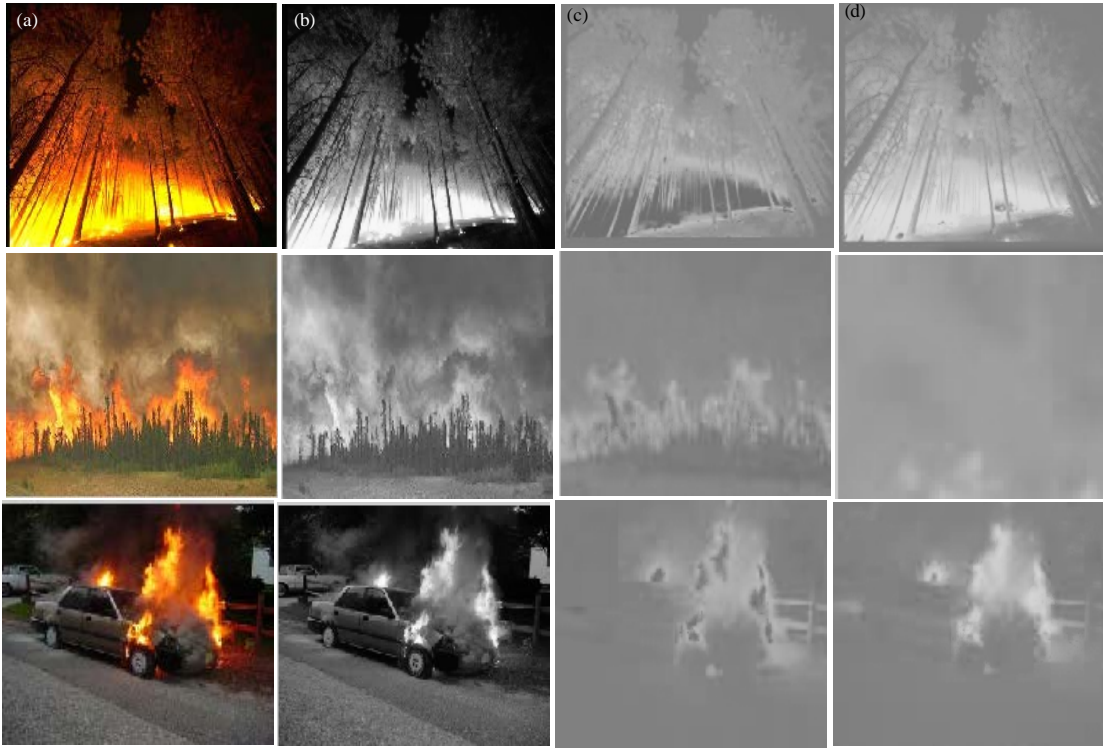


Fig. 6: Input image with L*, a* and b* components; a) Input RGB image; b) L* component of input image; c) a* component input image and d) b* component of input image

indicating b* as yellow color and negative value of b* indicating b* as an blue color. For analysis in CIE L*a*b* color space, it is necessary to convert RGB-L*a*b* color space.

Transformation from RGB-CIE L*a*b* color space results in an irregularly shaped gamut of colors and its shape is dependent on illumination condition. Although it has an advantage of color uniformity, the CIE L*a*b* color space does not have all the colors that a human being can feel as in XYZ color space.

Therefore, RGB is converted into XYZ color space and then in to CIE L*a*b* color space as shown in Eq. 11-15:

$$\begin{bmatrix} X \\ Y \\ Z \end{bmatrix} = \begin{bmatrix} 0.412453 & 0.35758 & 0.180423 \\ 0.212671 & 0.71516 & 0.072169 \\ 0.019334 & 0.119193 & 0.950227 \end{bmatrix} \begin{bmatrix} R \\ G \\ B \end{bmatrix} \quad (11)$$

$$L^* = \begin{cases} 116 \times (Y/Y_n)^{1/3} - 16 & \text{if } (Y/Y_n) > 0.008856, \\ 903.3 \times (Y/Y_n), & \text{otherwise} \end{cases} \quad (12)$$

$$a^* = 500 \times (f(X/X_n) - f(Y/Y_n)) \quad (13)$$

$$b^* = 200 \times (f(Y/Y_n) - f(Z/Z_n)) \quad (14)$$

$$f(t) = \begin{cases} t^{1/3}, & \text{if } t > 0.008856 \\ 70787 \times t + (16/116), & \text{otherwise} \end{cases} \quad (15)$$

where, X_n , Y_n and Z_n are tri-stimulus values of reference white colour. The value of L*, a* and b* components varies from 0-100,-110-110 and-110-110, respectively.

Rules in L*a*b* color space: In image analysis, the color information of the image is visualized through three channels i.e, L* channel, a* channel and b* channel. To analyze the chromatic characteristics of fire in L*a*b* color space, L*, a* and b* planes are separated from the input image as shown in Fig. 6. From Figure it is observed that L* component is higher compared to b* component and b* component is higher compared to a* component and hence L* component is greater than a* component. Figure 6 shows the value of L*, a* and b* components at the fire and non-fire region in the different locations of the input image. In CIE L*a*b* color space to increase the detection rate and to reduce the false alarm rate the statistical parameter called mean of the image in L* and b* plane is considered.

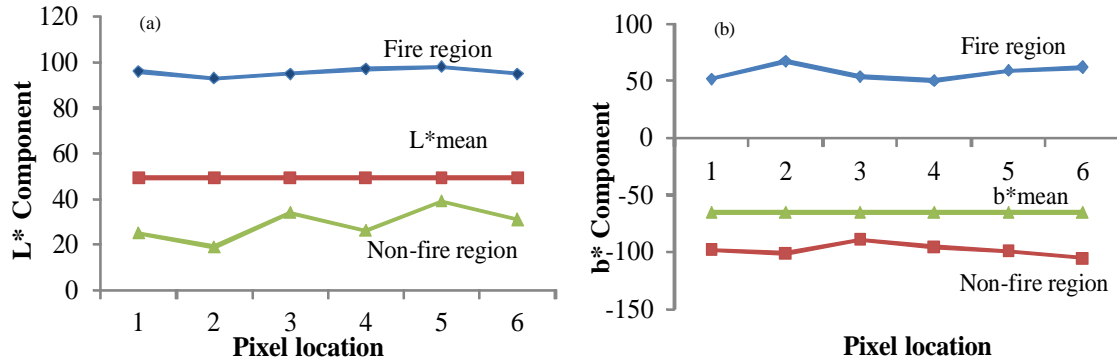


Fig. 7: a) Variation of fire and non-fire pixel intensity in L* plane along with L*_{mean} and b) Variation of fire and non-fire pixel intensity in b* plane along with b*_{mean}.

Since fire exists with high magnitude of illumination which exhibits the condition for the pixels in fire region but not in the non-fire region. In this color space b* plane encodes yellow color sensation more than other blue like dark colors. Since yellow is one of the major colors in fire which, visualizing it through digital camera, leads to the inclusion of statistical measure in b* plane called b*_{mean} of the image. This idea is depicted in Fig. 7 and it is observed that b* component is greater than b*_{mean} for the fire pixels and not for non-fire pixels.

The above mentioned observations which are verified over countless experiments with images containing fire regions are formulated as the following rule:

$$R_{LabI}(x, y) = \begin{cases} 1, & \text{if } L^*(x, y) > b^*(x, y) > a^*(x, y) \\ 0 & \text{otherwise} \end{cases} \quad (16)$$

$$R_{LabII}(x, y) = \begin{cases} 1, & \text{if } L^*(x, y) > L^*_{mean} \text{ and } b^*(x, y) > b^*_{mean} \\ 0 & \text{otherwise} \end{cases} \quad (17)$$

Where:

$L^*(x, y)$, $a^*(x, y)$ and $b^*(x, y)$ = The intensity of L*, a* and b* components in the corresponding plane

$R_{LabI}(x, y)$ and $R_{LabII}(x, y)$ = The pixels which satisfy the conditions given in Eq. 16 and 17

L^*_{mean} and b^*_{mean} = The mean value of pixel intensity in L* and b* plane respectively. Equation to calculate L^*_{mean} and b^*_{mean} is given in Eq. 18 and 19

$$L^*_{mean} = \frac{1}{M \times N} \sum_{x=1}^M \sum_{y=1}^N L^*(x, y) \quad (18)$$

$$b^*_{mean} = \frac{1}{M \times N} \sum_{x=1}^M \sum_{y=1}^N b^*(x, y) \quad (19)$$

Fire in L*a*b* color space is concluded by using the following expression:

$$R_{Lab}(x, y) = \begin{cases} 1(x, y), & \text{if } R_{LabI}(x, y) = 1 \text{ and } R_{LabII}(x, y) = 1 \\ 0 & \text{otherwise} \end{cases} \quad (20)$$

Where:

$R_{Lab}(x, y)$ = The segmented fire pixels in L*a*b* color space

$I(x, y)$ = The intensity of input RGB image at the location (x, y)

Performance in CIE L*a*b* color space: In CIE L*a*b* color space, fire pixels are analysed through the three channels of color space by taken in to account of statistical parameter (mean) of the image. The result of fire pixel segmentation in L*a*b* color space is shown in Fig. 8. It shows moderate results compared to other models discussed. In the fourth row of Fig. 8, white colored cloud is present in the input image which is also separated as fire region using the condition given in Eq. 20.

Analysis in YCbCr color space: In video and digital photographic system, YCbCr color space is used as a part of color image pipeline. In YCbCr color space, 'Y' is the luminance, 'Cb' is the chrominance blue and 'Cr' is the chrominance red components. In this color space, 'Cb' is

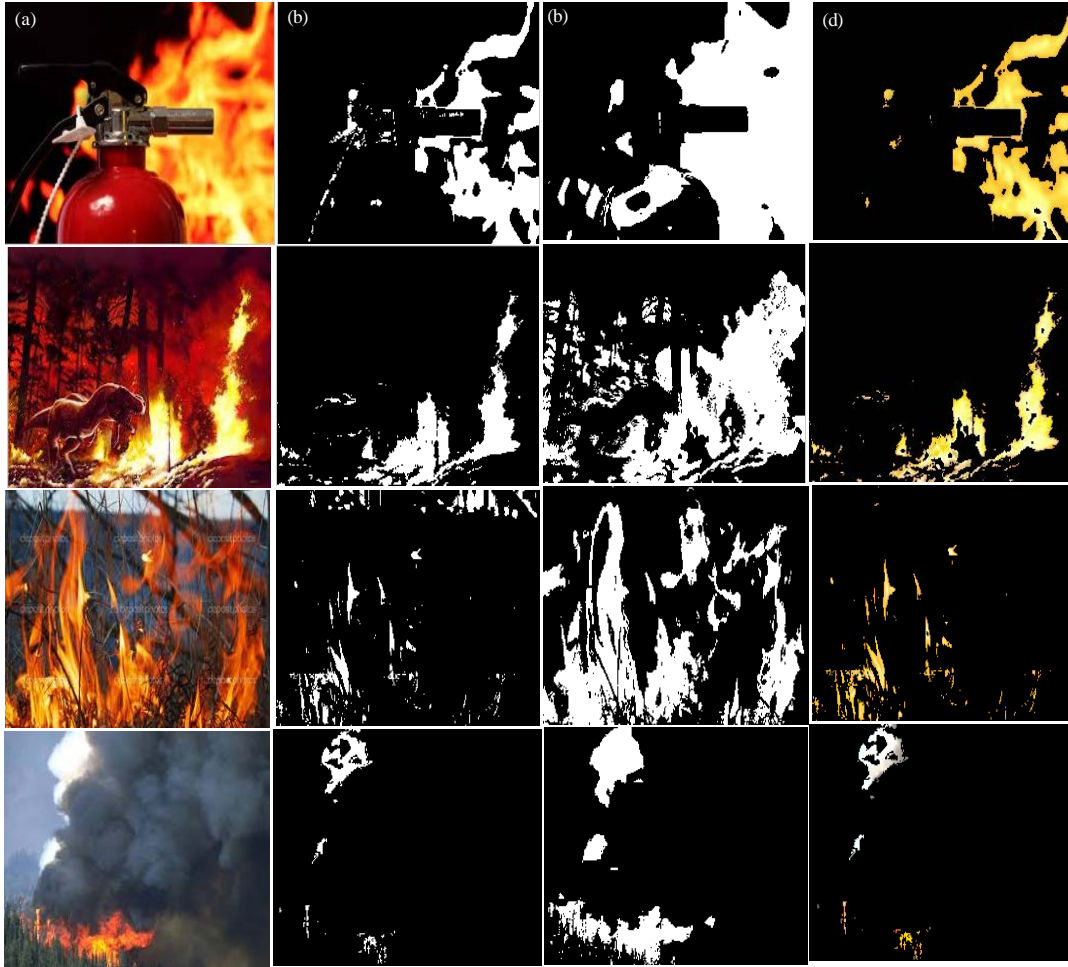


Fig. 8: Segmented fire region using CIE L*a*b* color space; a) input image; b) segmented fire region using Eq. 16; c) segmented fire region using Eq. 17 and d) segmented fire region using Eq. 20

blue minus luminance known as blue difference and ‘Cr’ is red minus luminance known as red difference. YCbCr is one way of encoding RGB information but it is not an absolute color space.

In YCbCr color space luminance information can be separated from the chrominance information. Hence, it can exhibit real performance when the illumination changes. Chrominance information is used in modelling the color of the fire rather than modelling its intensity. In YCbCr color space separation between intensity and chrominance is more discriminatory. Conversion from RGB into YCbCr color space is linear and it is given as:

$$\begin{bmatrix} Y \\ Cb \\ Cr \end{bmatrix} = \begin{bmatrix} 0.2568 & 0.5041 & 0.0979 \\ -0.1482 & -0.2910 & 0.4392 \\ 0.4392 & -0.3678 & -0.0714 \end{bmatrix} \begin{bmatrix} R \\ G \\ B \end{bmatrix} + \begin{bmatrix} 16 \\ 128 \\ 128 \end{bmatrix} \quad (21)$$

The range of ‘Y’ is [16,235], the ‘cb’ is [16, 240] and the range of ‘cr’ is [16, 240].

Rules in YCbCr color space: To perform analysis in YCbCr color space RGB image is converted in to the image in YCbCr color space using Eq. 21. Fire region is segmented from the input image in YCbCr color space using two steps. The first step is the segmentation of low temperature fire flame region and the second step is the segmentation of high temperature fire centre region. True fire region is obtained by adding the fire flame region and the fire centre region.

To segment the low temperature fire flame region, Y, Cb and Cr components of the fire image were separated as shown in Fig. 9. It is observed that the brightness of Y component is greater than Cb component. But in the non-fire region, Cb component is greater than Y component (Horng *et al.*, 2005). Hence, it is concluded that Y component is greater than Cb component at low temperature fire flame region. Very high temperature exists at the centre region of fire which exhibits white color. To

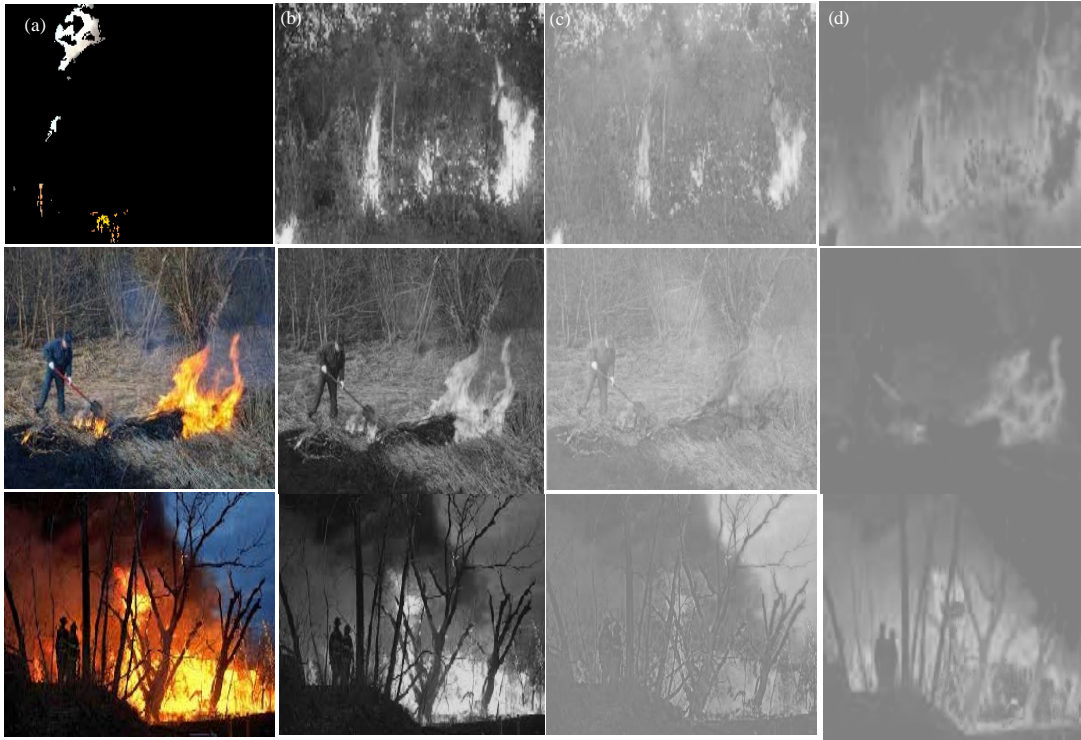


Fig. 9: Input image with Y, U and V components; a) Input image; b) Y component of input image; c) Cb component of input image and d) Cr component of input image

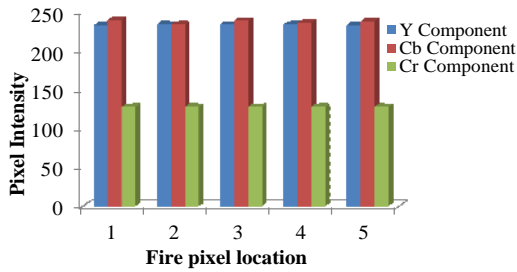


Fig. 10: Y, Cb and Cr components of fire pixels at the fire centre region

segment the high temperature fire centre region, the luminance (Y) and chrominance components (Cb and Cr) are calculated from the fire centre region. This shows that the luminance component is greater than the chrominance red component (Cr) but it is less than the chrominance blue component (Cb).

To explain this idea many high temperature fire images are collected from the internet and their centres are analyzed. Then bar chart is drawn between the pixel at the centre of the fire at different spacial locations and its corresponding intensity as shown in Fig. 10. While

segmenting the fire centre, based on luminance, some of the white colored regions like clouds and smokes are also segmented from the input image.

To overcome this problem, the texture of the fire region is also considered. Fire and the non-fires like clouds have different textures. Texture of the fire region can be defined by the statistical parameters of the image like mean, median, standard deviation, variance etc. To get better performance standard deviation of the image in Cr plane is incorporated, i.e., Crstd. All the above observations can be explained as the following rules:

$$R_{YCbCrI}(x, y) = \begin{cases} 1 & \text{if } Y(x, y) > Cb(x, y) \\ 0 & \text{otherwise} \end{cases} \quad (22)$$

$$R_{YCbCrII}(x, y) = \begin{cases} 1 & \text{if } Cb(x, y) \geq Y(x, y) > Cr(x, y) \\ 0 & \text{otherwise} \end{cases} \quad (23)$$

$$R_{YCbCrIII}(x, y) = \begin{cases} 1 & \text{if } Cr(x, y) < \tau_{Crstd} \\ 0 & \text{otherwise} \end{cases} \quad (24)$$

where, $R_{Ycbri}(x, y)$, $R_{Ycbrii}(x, y)$ and $R_{Ycbriii}(x, y)$ are the pixels which satisfy the conditions given in Eq. 22-24



Fig. 11: Samples from an image set used to find the value of τ

respectively. ‘ τ ’ is constant and the value of ‘ τ ’ is determined by the analysis of the image set consisting of 1000 images. Figure 11 shows a few samples from this set. Furthermore, the images are selected so that fire centre like colored objects is also included in the set. Based on the analysis conducted on the image set, τ value is selected as 7.4. cr_{std} is the standard deviation of the input image in Cr plane and is calculated using Eq. 25:

$$Cr_{std} = \sqrt{\frac{1}{M \times N} \sum_{x=1}^M \sum_{y=1}^N (Cr(x,y) - Cr_{mean})^2} \quad (25)$$

Where:

- $M \times N$ = The total number of pixels in the input image
- $Cr(x, y)$ = The Cr value of the pixel positioned at location (x, y)
- Cr_{mean} = The mean value of the Cr plane of the input image and is given in Eq. 26:

$$Cr_{mean} = \frac{1}{M \times N} \sum_{x=1}^M \sum_{y=1}^N Cr(x,y) \quad (26)$$

Finally, the true fire region (including both low temperature and high temperature) is obtained by using the following rule:

$$\begin{cases} 1(x,y) & \text{if } R_{YCbCrI}(x,y) = 1 \text{ or } R_{YCbCrII}(x,y) = 1 \\ & \text{and } R_{YCbCrIII}(x,y) = 1 \\ 0 & \text{otherwise} \end{cases} \quad (27)$$

Where:

- $R_{YCbCr}(x, y)$ = The pixel which is segmented as true fire pixel in YCbCr color space
- $I(x, y)$ = The intensity of the input RGB image at the location (x, y)

Performance in YCbCr color space: Analysis in YCbCr color space produces good results than other color spaces, because it is more robust to the illumination changes. With the derived set of rules in YCbCr color space given in Eq. 22-24 and 27, one can classify whether a given pixel is true fire pixel or not. Figure 12 shows the result of the fire pixel segmentation in YCbCr color space.

Figure 12b shows how low temperature fire flame region is segmented from the input image using Eq. 17. Figure 12c shows the high temperature fire centre region segmented from the input image which is the pixel common to those pixels satisfying Eq. 18 and 19. At last the true fire region is obtained from the combination of both the low temperature fire flame region and high temperature fire centre region as shown Fig. 12d. Row 1 and 2 of Fig. 12 show high temperature fire with the white colored fire centre. In such case, the white colored centre region is not segmented using the condition given in Eq. 22. At the same time the centre pixels satisfy the condition given in both Eqs. 23 and 24 and is segmented as shown in Fig. 12c. Row III-V of Fig. 12 do not contain high temperature fire centre for visualization and hence no pixels are segmented as shown in Fig. 12c. Figure 12d shows the true fire pixels including both low temperature fire flame and high temperature fire centre.

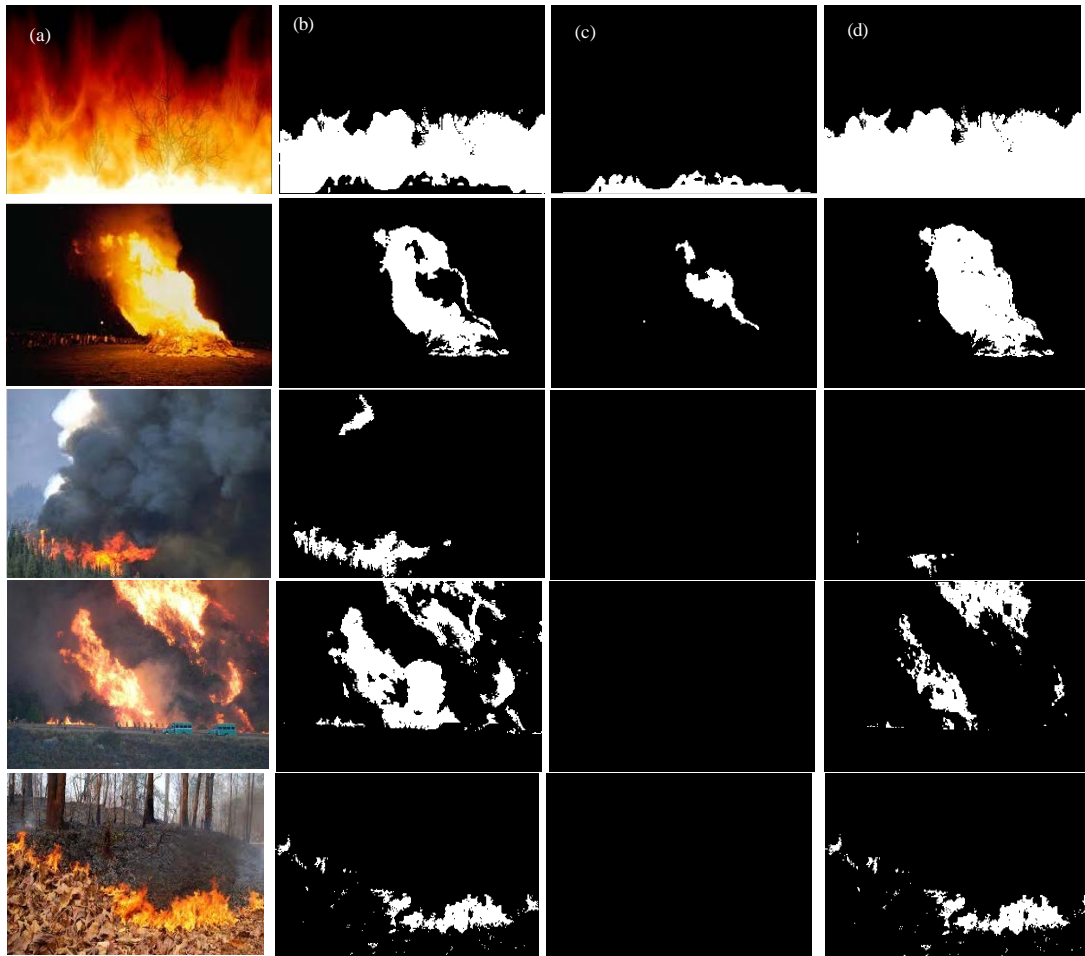


Fig. 12: Results observed in YCbCr color space; a) Input image; b) Fire pixels segmented using Eq. 22; c) Fire pixels segmented using Eq. 23 and 24 and d) Fire pixels segmented using Eq. 27

Performance evaluation: The performance of the fire pixel classifier is analyzed by generating different rules based on statistical image parameters in each color spaces. Figure 13 shows the result of fire pixel segmentation in RGB, YUV, CIE L*a*b* and YCbCr color spaces. During the analysis more than 1000 color images of size 256×256 are used which are totally different from the sets used for creating the fire rules in each color model. The set consists of 700 images which contain flame and the rest is a collection of the images with fire colored non-fire objects like sun, apple, red colored car etc. Almost all the video fire detection systems use RGB color space because all the visible range cameras have sensors detecting video in RGB format. Even though image analysis in RGB color space is simple, it is inaccurate in most of the situations. Also, it does not respond accurately when the background illumination changes since luminance and chrominance informations are mixed in RGB color space.

In YUV color space, luminance information (Y) is separated from chrominance information (U and V). It does not differentiate fire colored artificial light sources from fire, even by incorporating the texture feature using statistical parameters (Ymean, Vstd). Also, the centre region of a high temperature fire image is not segmented using YUV color space Marbach *et al.* (2006) used static feature as color and dynamic feature as flickering for fire detection. Here color-based segmentation is done in YUV color space that missed centre fire region. In L*a*b* color space luminance information is separated from chrominance information. By making the use of statistical parameters (L*mean and a*mean), it can discriminate fire and fire-like light sources. But the centre region of high temperature fire is not segmented (Celik, 2010).

Analysis in YCbCr color space shows better results than the other color spaces. This can separate both low temperature fire flame and high temperature fire centre. Also performance improvement is expected since YCbCr



Fig. 13: Result of fire pixel segmentation in various color spaces; a) RGB; b) YUV; c) CIE L*a*b* and d) YCbCr

color space has the ability of discriminating luminance information from chrominance information. Since without effect of luminance, the chrominance information dominantly represents the information, the chrominance-based rules and the color model defined in the chrominance plane are more descriptive of the fire behavior. Celik *et al.* (2006) used YCbCr color space for detecting the fire in videos along with the statistical parameters. But it separates only low temperature fire flame regions but not the high temperature fire centre region.

Three different measures were used to evaluate the performance of fire detection system in various color spaces. The detection rate is defined as the number of pixels that are correctly detected as fire color pixels over the total number of fire pixels.

The false positive rate is defined as the number of non-fire pixels that are detected incorrectly as fire pixels over the total number of non-fire pixels. The false negative rate is defined as the number of fire color pixels that are detected incorrectly as non-fire color pixels over the total number of fire pixels:

$$\text{Detection rate(D)}(\%) = \frac{\text{No. of pixels that are correctly detected as fire pixels } (N_{ff})}{\text{Total no. of fire pixels } (N_f)} \times 100$$

$$\text{False Positiverate(FP)}(\%) = \frac{\text{No. of non fire pixels that are incorrectly detected as fire pixels } (N_{nf})}{\text{Total no. of fire pixels } (N_n)} \times 100$$

$$\text{False negative rate(FP)}(\%) = \frac{\text{No. of fire pixels that are incorrectly detected as non fire pixels } (N_{nf})}{\text{Total no. of fire pixels } (N_f)} \times 100$$

From Table 2, it is concluded that YCbCr color space has high detection rate, low true positive and low false positive rate. Since YCbCr color space is idle to illumination changes it can be used for real time fire detection applications.

Table 2: Performance of fire pixel segmentation in various color spaces

Color space	D (%)	FP (%)	TP (%)
RGB	73.42	18.36	3.69
YUV	92.46	3.60	5.95
CIE L*a*b*	96.38	4.55	3.26
YCbCr	99.10	1.28	0.37

CONCLUSION

Color and texture are the static features of fire that plays major role in fire detection techniques. Color-based detection is the basic detection step in video fire detection systems; it is be used by almost all the fire detection systems. Even though the camera is in dynamic conditions, the color and texture based detection techniques have been applied. Also, by making the camera to move, it is possible to increase the area covered by the camera.

The performance of fire image segmentation technique based on static characteristics is analyzed in RGB, YUV, CIE L*a*b* and YCbCr color spaces. RGB color space-based segmentation technique is not complex but its detection rate is very less when the system is used for outdoor applications. YUV and CIE L*a*b* color space-based segmentation technique is guaranteed to be used under different climatic conditions but it is not able to segment the fire centre pixels. But by incorporating statistical image parameters in YCbCr color space, betterment of the fire detection system is achieved. Among all the color spaces discussed, YCbCr color space effectively segments the true fire region effectively. YCbCr color space- based technique not only separates low temperature fire flame pixels but also separates high temperature fire centre pixels by taking into account of the statistical parameter of the fire image in YCbCr color space (standard deviation). The analysis is carried out on three set of images. The first set contains fire. The second set contains fire-like regions. The third set contains fire centre-like regions. The results show that YCbCr based method can achieve a high detection rate compared to the other methods. In future along with the static color feature dynamic features of fire such as flickering, movement and growth are also considered.

REFERENCES

Celik, T., 2010. Fast and efficient method for fire detection using image processing. *ETRI J.*, 32: 881-890.

Celik, T., H. Demirel and H. Ozkaramanli, 2006. Automatic fire detection in video sequences. *Proceedings of the 14th European Conference on Signal Processing*, September 4-8, 2006, IEEE, Florence, Italy, pp: 1-5.

Celik, T., H. Ozkaramanli and H. Demirel, 2007. Fire pixel classification using fuzzy logic and statistical color model. *Proc. IEEE Int. Conf. Acoustics Speech Signal Process.*, 1: 1205-1208.

Chen, T., P. Wu and Y. Chiou, 2004. An early fire-detection method based on image processing. *Proc. Int. Conf. Image Process.*, 3: 1707-1710.

Elik, T.C. and H. Demirel, 2009. Fire detection in video sequences using a generic color model. *Fire Safety J.*, 44: 147-158.

Hong, W.B., J.W. Peng and C.Y. Chen, 2005. A newimage-based real-time flame detection method using color analysis. *Proceedings of the International Conference on Networking, Sensing and Control*, March 19-22, University Marriott Park Hotel, Tucson, USA., pp: 100-105.

Jin, H. and R.B. Zhang, 2009. A fire and flame detecting method based on video. *Proc. 8th Int. Conf. Mach. Learn. Cybernet.*, 4: 2347-2352.

Ko, B.C., K.H. Cheong and J.Y. Nam, 2009. Fire detection based on vision sensor and support vector machines. *Fire Saf. J.*, 44: 322-329.

Marbach, G., M. Loepfe and T. Brupbacher, 2006. An image processing technique for fire detection in video images. *Fire Saf. J.*, 41: 285-289.

Patel, P. and S. Tiwari, 2012. Flame detection using image processing techniques. *Int. J. Comput. Appl.*, 58: 13-16.

Toreyin, B.U., Y. Dedeoglu and A.E. Cetin, 2005. Flame detection in video using hidden markov models. *Proc. IEEE Int. Conf. Image Process.*, 2: 1230-1233.

Toreyin, B.U., Y. Dedeoglu, U. Gueduekbay and A.E. Cetin, 2006. Computer vision based method for real-time fire and flame detection. *Pattern Recognition Lett.*, 27: 49-58.

Vipin, V., 2012. Image processing based forest fire detection. *Int. J. Emerging Technol. Adv. Eng.*, 2: 87-95.

Xie, M., J. Wu, L. Zhang and C. Li, 2009. A novel boiler flame image segmentation and tracking algorithm based on YCbCr color space. *Proceedings of the International Conference on Information and Automation*, June 22-24, 2009, IEEE, Zhuhai, China, ISBN: 978-1-4244-3608-8, pp: 138-143.